Thermomechanical Implications of X-Point Sweeping for Divertor Target Elements

E. Zolti
Max Planck Institute für Plasmaphysik, Garching, bei Muenchen, FRG

1. INTRODUCTION

The sweeping of the separatrix on the divertor target elements has been proposed to reduce the erosion on the protection surface and to attenuate the thermomechanical effects of the highly localized peak surface heat fluxes [1].

For the sweeping to be feasible possible frequencies and amplitudes, thermomechanically favourable, are to be compatible with electrotechnical requirements (e.g. limited eddy currents power losses for acceptable additional power supply and heat removal in the superconducting coils) and with divertor layout limitations. A limit on the amplitude is anyway set by the minimum distance of ~50 cm between the two peak load areas (fig. 1).

The objective of this study is a first quantitative assessment of the thermal and mechanical implications of the X-point sweeping for different frequencies and amplitudes. It addresses the divertor design with TZM heat sink structure, brazed graphite tiles and 10 MW/m^2 peak surface heat load (fig. 1), which is among the concepts mainly studied for NET at present.

2. ANALYSIS PROCEDURE AND ASSUMPTIONS

For the objectives of this preliminary study it is sufficient to consider only one of the two peaks of the heat flux distribution (fig. 1) and thus the zone at the intersection with the outboard separatrix, showing the highest thermal load.

As the X-point sweeps, each cross section experiences periodic heat flux variations with different time evolutions, depending on its location in this area and on the sweeping wave characteristics, as frequency f, amplitude A and linear or sinusoidal shape.

Fig. 2 shows the heat flux histograms for 1 pulse including typical evolutions during one sweeping cycle at the locations of the sweeping center, $q_C(t)$ and edge, $q_A(t)$, assuming linear or sinusoidal sweeping wave. The coolant conditions are given in fig. 1 and the volumetric heat generation is 15 W/cm^3 for TZM and 5 W/cm^3 for graphite.

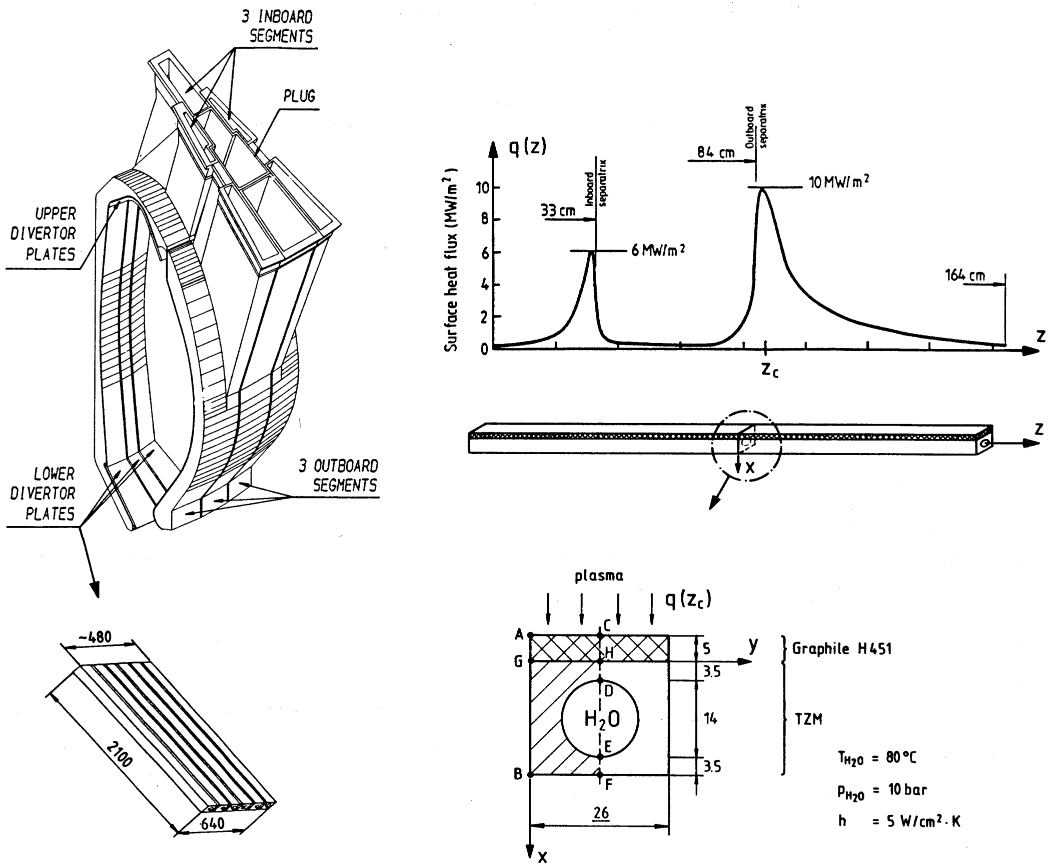

Fig. 1 : Surface heat flux distribution, geometry and materials of divertor target

The geometric model (i.e. the finite element discretization of the zone ACFB of fig. 1) and the boundary displacement conditions, including the generalized plain strain conditions in the longitudinal (z) direction are the same as the problem described in [3]. The material properties are taken from [4] for TZM and [5] for the graphite H451. Based on this 2-D (x,y) model, a set of transient calculations of temperatures, stresses and stress ranges for the cross sections at the locations C and A_{20}, for frequencies 0, 0.01, 0.1 and 1 Hz, and for amplitudes 10, 20, 30 and 45 cm has been carried out, and the stress ranges in the TZM structure evaluated with respect to thermal fatigue. Furthermore, to quantify possible thermal longitudinal effects, also a 2 dimensional analysis with 0.01 Hz and 20 cm has been performed in the plane x, z for a sufficient extended area under the peak heat load.

All the calculations have been carried out through the computer code IAFETIN [2].

3. RESULTS

A typical time evolution of the temperatures of graphite at the hottest (T_A) and coldest (T_H) location and of TZM or brazing joint at the hottest location (T_G) of the

Fig. 2 : Assumed heat flux distribution and sweeping waves

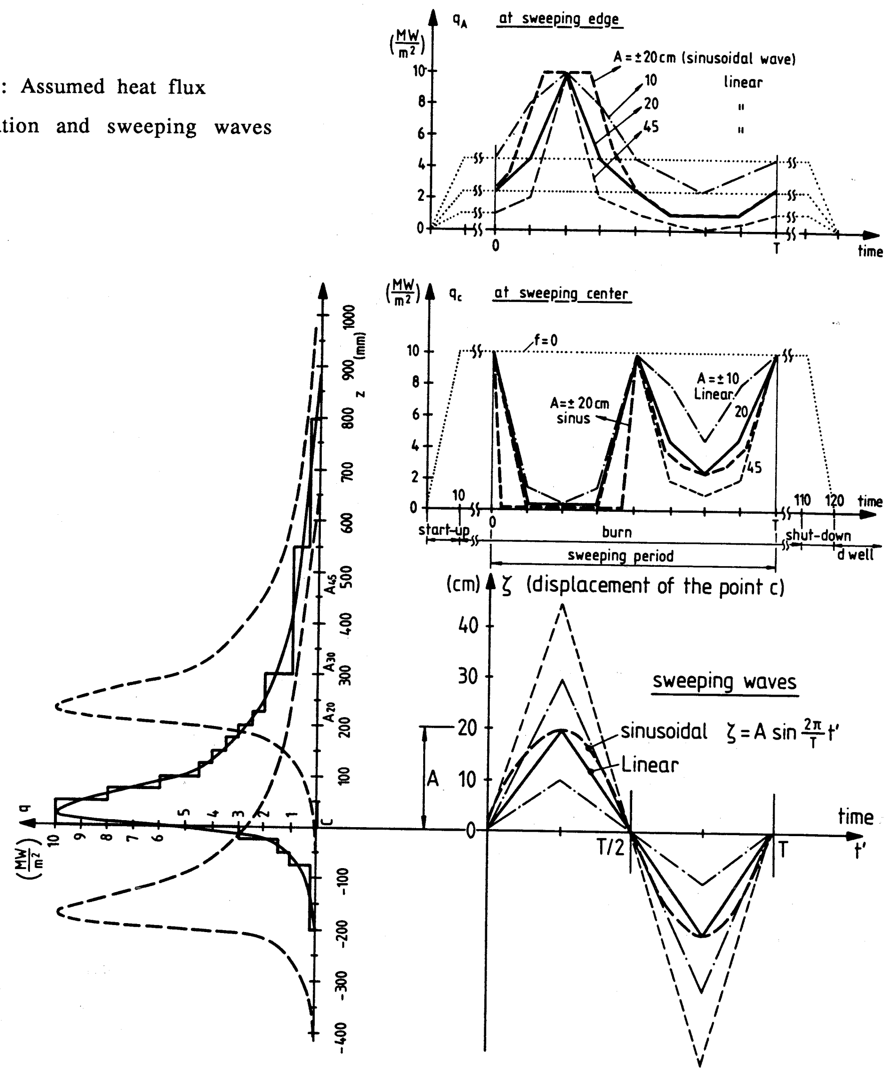

sweeping center cross section is given in figs. 2 and 3 for the case of f = 0.1 Hz, A = ±20 cm and linear sweeping wave. Also given are the stresses in TZM at the coolant channel location closest to the plasma (point D in fig. 1). Since $\sigma_y{}^D$ is the highest tensile stress and the other components $\sigma_x{}^D$ and $\sigma_z{}^D$ much smaller, the ranges of the stress time variation $\Delta\sigma_y{}^D$ are the most relevant for crack propagation and can be considered as representative measure for fatigue damage evaluation.

As shown in fig. 4 in addition to the stress range $\Delta\sigma^I$ due to the main pulse two more ranges $\Delta\sigma_y{}^{II}$ and $\Delta\sigma_y{}^{III}$ are introduced in each sweeping cycle and their fatigue damage contributions sums to that of $\Delta\sigma^I$.

The dependence of the temperatures T_A, T_H, T_G on the frequency and amplitude for the case of linear wave and sweeping center location is summarized in fig. 5 and that of the stress ranges $\Delta\sigma^I$ and $\Delta\sigma^{II}$ and $\Delta\sigma^{III}$ in fig. 6.

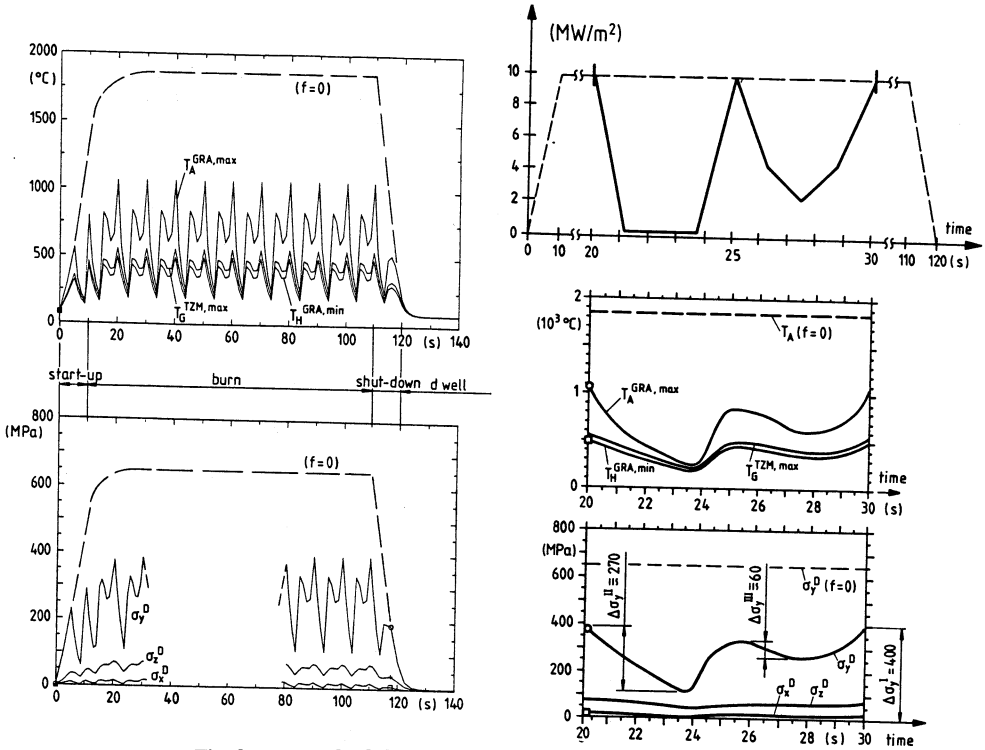

Fig. 3 : Results for f=0.1 Hz, A=±20 cm, sweeping center, linear wave

As compared to the static case the peak values of the graphite surface temperature decrease with increasing frequency and amplitude, e.g. by a factor of about 2 at 0.1 Hz and ±45 cm.

Similar tendence, but with slightly lower rate, show the minimum graphite temperature T_H and the maximum TZM temperature T_G.

In case of no sweeping actuation during start-up and shut-down phase, the peak temperatures are higher than those given in fig. 5 arising at the beginning or at the end of the burn time.

The stress range $\Delta\sigma^I$, due to the main pulse, decreases with increasing amplitude and frequency up to 0.1 Hz. At higher frequency $\Delta\sigma^I$ decreases further up to a factor of about 2 at 1 Hz, if the sweeping is actuated also before and after the burn time. Otherwise it decreases up to 0.1 Hz, and then remains constant, being determined by the peak stresses present at the end of the start-up or at the beginning of the quench phase. The stress range $\Delta\sigma^{II}$ due to the first sweeping excursion decreases also with increasing frequency, but has no or little dependence on the amplitude. The stress range $\Delta\sigma^{III}$ due to the second sweeping excursion decreases more rapidly with increasing frequency, becoming negligible at f = 1 Hz, but increases clearly with increasing amplitude.

Improving the thermal conductivity of the protection, e.g. using a c/c composite, results in reduced surface temperature, but also in higher stress variations in the TZM structure. Analogous effects have been found by increasing the coefficient of

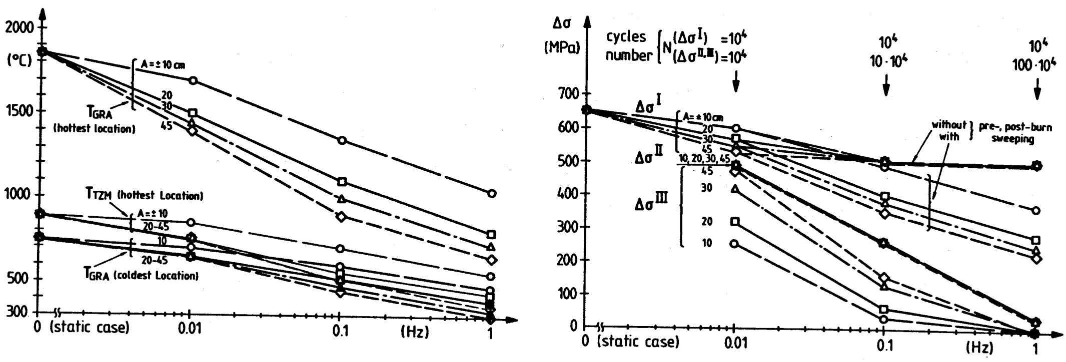

Fig. 4 : Frequency dependence of temperatures and stress ranges at sweeping center (linear wave)

convective heat transfer to the coolant, or reducing the graphite thickness and thus the thermal inertia.

As compared to the linear sweeping wave, the sinusoidal wave has unfavourable implications (i.e. higher temperatures, stresses and stress ranges) at the edge location and favourable at the center as expected on the basis of the longer loading times at the edge and of the shorter times at the center. However at the edge locations the peaks arise only once per sweeping cycle and a comparison with the situation at the center from the erosion standpoint is to be based on the time integration of the surface temperature effects. The additional fatigue damage at the edge is negligibly small.

The quantification of the individual fatigue damage contributions due to $\Delta\sigma^{I}$, $\Delta\sigma^{II}$ and $\Delta\sigma^{III}$ and thus of the total damage (D) can be based on the usual linear fraction rule :

$$D = \Sigma_i \, (N_i/N_{allow})$$

where i = I, II, or III index of loading condition.

N_{allow} = allowable number of cycles corresponding to the $\Delta\sigma^{(i)}$ stress range at the maximum local temperature.

$N_i(f)$ = number of cycles of the loading condition i.

The allowable number of cycles are determined by the fatigue behaviour of the TZM represented by fatigue curves $\Delta\sigma = f\,(N_{allow}, \text{Temp.})$. Since these curves are not yet available, a detailed determination of the thermal fatigue damage D is presently not possible. A first indication on the fatigue implications of the X-point sweeping can however be obtained assuming on hypothetical design fatigue curve using the scarse failure data reported in the literature (e.g. [4]) with a safety factor of 2 and considering only the relative fatigue damage with respect to the value of the static case.

With these assumptions it resulted that :

- the fatigue damage at f = 0 is so high that the considered TZM divertor element is clearly to be excluded for operation at 10 MW/m^2 for 10^4 cycles without sweeping.

- With increasing frequency and amplitude the damage contribution D^I of the stress range $\Delta\sigma^I$ (due to the main pulse) decreases, being reduced by several orders of magnitude at 0.1 Hz and higher frequencies. It is to be noted, however, that in the case of no sweeping actuation during start-up and shut-down phase this contribution alone would be still excessive even at highest frequencies.
- The fatigue damage contributions due to the sweeping additional stress variations $\Delta\sigma^{II}$ and $\Delta\sigma^{III}$ are considerable at 0.01 Hz and highest amplitudes, but decrease strongly with increasing frequency, despite the larger number of cycles. From 0.1 Hz they are practically negligible.

4. CONCLUSIONS

The results of the parameteric analysis of the X-point sweeping for the specific case of divertor target with TZM as heat sink structure, and brazed graphite protection clearly indicate increasing thermomechanical advantages with increasing frequency and amplitude both at sweeping center- and edge locations.

The sweeping parameters :

- frequency	around 0.1 Hz
- amplitude	±20 to ±30 cm (on divertor surface)
- pre- and post-sweeping	few seconds (e.g. 5) before and after burn time

are suggested from the thermomechanical viewpoint for first orientation in sweeping system design.

These parameters seem to comply also with the electrotechnical requirements (e.g. eddy current power losses and heat removal in the superconducting coils) and possible amplitude limitations for divertor layout reasons.

The thermomechanical optimization of the X-point sweeping will depend on the specific design solution (geometry, materials) and on the allowable temperatures at the graphite surface and at the brazing joint. Anyway for a realistic description of the material behaviour under cyclic loading in terms of fatigue curve or fracture mechanics properties is indispensable.

REFERENCES

[1] ITER-Concept Definition, IAEA, ITER-1, October 1988.

[2] E. Zolti, Das Finite Elemente Rechenprogramm IAFETIN fuer thermoinelastische Analyse von 2D Strukturen.
Teil 2. Benutzerhandbuch, INTERATOM Report ITB 54.089838 (1984).

[3] E. Zolti, Thermomechanical design evaluation and material properties requirements for NET divertor elements, J. of Nucl. Mat. 155-157 (1988) 386-391.

[4] R.E. Gold, D.L. Harrod, Refractory metal alloys for fusion reactor applications, J. of Nucl. Mat. 85-86 (1979) 805-815.

[5] W.M. Stacey, USA FED-INTOR/82-1, Georgia Institute of Technology.